Combining the eXtended Finite Element Method with Virtual Crack Closure Technique and Cohesive Surface Modeling to simulate delamination migration in cross-ply laminates

Nelson V. De Carvalho, Ronald Krueger

National Institute of Aerospace, Hampton, Virginia

Abstract: *Using recently developed benchmarks, the performance of the eXtended Finite Element Method (XFEM), as implemented in Abaqus/Standard, is assessed and its main features highlighted. Subsequently, a strategy is proposed to model delamination migration using Abaqus/Standard that combines: the Cohesive Surface (CS) formulation and/or the Virtual Crack Closure Technique (VCCT) to model delamination with XFEM to capture migration. Finally, the proposed strategy is applied to model the Delamination Migration (DM) test and the results obtained are compared to experiments.*

***Keywords**: Composites, Crack Propagation, Damage, Delamination, Experimental Verification, Failure, Fracture.*

1. Introduction

Delamination is one of the most critical damage mechanisms in tape laminates. It has been successfully modeled using techniques such as the Virtual Crack Closure Technique (VCCT) or Cohesive Surface/Cohesive Elements (CS/CE). However, delaminations often migrate via matrix cracks from one interface to the other. Capturing this migration process is crucial to accurately model damage progression in composite structures.

Both VCCT and CS/CE require the mesh to conform to the crack path, which is generally the case when modeling the interface between plies of different orientations. However, the path and location of the matrix cracks associated with the migration process is not known beforehand. Therefore, these techniques are, in general, not sufficient. To model crack growth in a mesh-independent fashion, without requiring “a priori” knowledge of the crack path, Abaqus/Standard offers the eXtended Finite Element Method (XFEM). In the present work, VCCT and/or CS are combined with XFEM to model delamination migration in Abaqus/Standard 6.13.

The work here presented focuses on the application of the XFEM method, and its combination with other modeling techniques, as available in Abaqus/Standard 6.13. The works from (Belytschko, 1999) and (Song, 2006) are recommended to the reader interested in the details of XFEM or the Phantom Node Method (PNM), on which the crack propagation technique implemented in Abaqus/Standard is based. In the present work, a brief description of some of the options available to model crack propagation with XFEM in Abaqus/Standard 6.13 is first provided in Section 2. In Sections 3 and 4, the accuracy of XFEM is evaluated using recently developed benchmarks, as discussed in detail in (Krueger, 2008) and (Krueger, 2012). These benchmarks were designed to allow the assessment of analysis tools used to model straight crack propagation under Mode I and Mixed Mode I/II conditions, using the Double Cantilever Beam (DCB) and the Mixed Mode Bending specimens, respectively. In Section 5, a methodology is proposed to capture delamination migration using Abaqus/Standard. This methodology is assessed by modeling the Delamination Migration (DM) test (Ratcliffe, 2012) and comparing the computed results to experiments. A discussion of the results is presented in Section 6, and a summary of the main conclusions is provided in Section 7.

2. XFEM and crack propagation modeling in Abaqus/Standard

In Abaqus/Standard, to enable an XFEM crack to initiate/grow in a given area of the model, the elements in that area need to be enriched with the XFEM formulation. This is done using the keyword, '`*enrichment`'. In each enriched area, only one XFEM crack can initiate/propagate, unless multiple cracks initiate/propagate simultaneously (in the same increment).

Abaqus/Standard provides two options to model the propagation of an XFEM crack. In the first option, here referred to as XFEM-CS, a damage initiation criterion is used to determine failure. When failure is detected, a cohesive segment is inserted using the XFEM framework, and opens according to a prescribed traction-separation law. Different damage initiation criteria and traction-separation laws can be selected or defined by the user. In the present work two different damage initiation criteria are used, the quadratic stress (QUADS) criterion and maximum principal stress criterion (MAXPS). The quadratic stress (QUADS) criterion is given by

$$\left\{\frac{\langle t_n \rangle}{t_n^0}\right\}^2 + \left\{\frac{t_s}{t_s^0}\right\}^2 + \left\{\frac{t_t}{t_t^0}\right\}^2 = 1, \tag{1}$$

where the operator $\langle . \rangle$ is defined as $\langle x \rangle = \max\{0, x\}$, t_n, t_s and t_t are the normal and shear tractions at the interface, and the constants t_n^0, t_t^0 and t_s^0 are the peak values of the interface tractions when the separation is either purely normal to the interface or purely in the first or the second shear direction, respectively. This criterion is used in the Double Cantilever Beam (DCB) and Mixed Mode Bending (MMB) benchmarks, where the direction of the crack is prescribed, and therefore the crack plane is known and fixed. In the DM test, a maximum principal stress criterion is used, providing not only the damage onset but also the crack orientation. By default, in XFEM-CS, failure of each element is determined by assessing the damage initiation criterion at the centroid of the element. In Abaqus/Standard 6.13, this can be changed by the user through the option '`position = cracktip`', in the keyword '`*Damage Initiation`'. In this case, after a crack is onset, the failure of the element ahead of the crack is determined by the stress at the crack tip, which has been extrapolated from the integration points. The traction-separation response is modeled using a standard bi-linear law with a mixed mode response defined by the BK criterion (Benzeggagh, 1996):

$$G_c = G_n^c + (G_S^c - G_n^c)\left\{\frac{G_S}{G_T}\right\}^{\eta}, \tag{2}$$

where G_S is the sum of the shear components of the energy release rate $G_S = G_s + G_t$, and the total energy release rate G_T is the sum of opening and shear components $G_T = G_n + G_s$. The exponent η is a constant determined by fitting Equation 2 to the experimental fracture toughness data.

The second option, here referred to as XFEM-VCCT, uses a stress or strain based initiation criterion to determine onset, while propagation is modeled by comparing the energy release rates determined at the crack tip using VCCT to a given fracture criterion. If the XFEM crack has onset or is predefined, as in the DCB and MMB specimens, no damage initiation criterion is needed. In the present work, the fracture criterion used was the BK criterion given by Equation 2.

In the following sections, these two options, XFEM-CS and XFEM-VCCT, and some of its features are assessed using DCB (Mode I) and MMB (Mode I/II) benchmarks. The goal is to first gain an understanding of the overall performance of the XFEM implementation in Abaqus/Standard 6.13.

3. XFEM assessment: DCB benchmark

In this section, the XFEM capability to model crack propagation is assessed using the DCB benchmark developed in (Krueger, 2008). A brief description of the numerical model and procedure used to obtain the benchmark is provided in the next section.

3.1 Benchmark

Figure 1 illustrates the reference numerical model used to obtain the DCB benchmark, including dimensions, material properties and boundary conditions (Krueger, 2008).

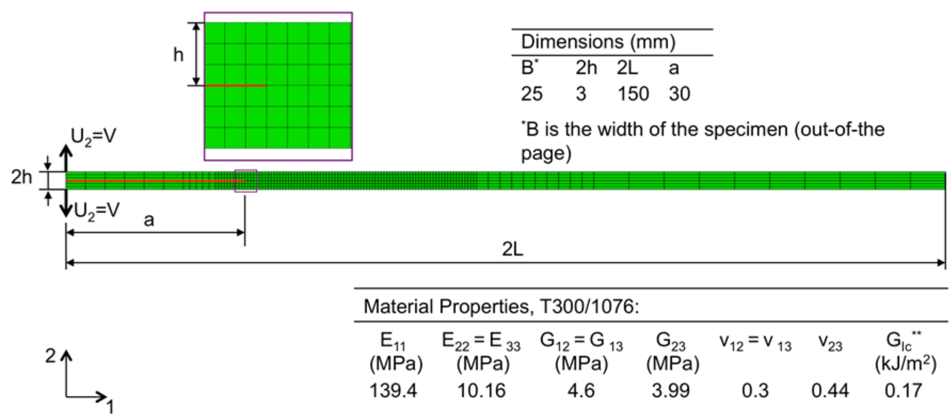

Dimensions (mm)			
B*	2h	2L	a
25	3	150	30

*B is the width of the specimen (out-of-the page)

Material Properties, T300/1076:						
E_{11} (MPa)	$E_{22} = E_{33}$ (MPa)	$G_{12} = G_{13}$ (MPa)	G_{23} (MPa)	$\nu_{12} = \nu_{13}$	ν_{23}	G_{Ic}** (kJ/m^2)
139.4	10.16	4.6	3.99	0.3	0.44	0.17

**Obtained from T300/914C

Figure 1. Numerical model and material properties used to obtain the DCB benchmark proposed in (Krueger, 2008).

To create the benchmark results, two-dimensional finite element models are used for simulating DCB specimens with different delamination lengths. For each delamination length modeled, the load and the displacement are monitored. The total strain energy release rate, G_T, is calculated for a fixed applied displacement. It is assumed that the delamination propagates when the computed energy release rate, G_T, is equal to the fracture toughness $G_c = G_{Ic}$. Finally, the critical loads and displacements for each delamination length are calculated from:

$$P_{crit} = P\sqrt{\frac{G_c}{G_T}}, \qquad V_{crit} = V\sqrt{\frac{G_c}{G_T}}. \tag{3}$$

The path connecting the critical values in a load/displacement plot is defined as the benchmark. It is assumed that during the automated propagation, the analysis has to follow the critical path. More details of the benchmark development and an assessment of the VCCT implementation in Abaqus are presented in (Krueger, 2008).

3.2 XFEM DCB

Figure 2 shows three models with increasing number of Degrees of Freedom (DoF) and decreasing element size, M0 to M2, used to assess the performance of XFEM as implemented in Abaqus/Standard 6.13. The dimensions, boundary conditions and material properties are identical to those used in the benchmark problem, Figure 1. The initial XFEM crack and mesh were defined such that the XFEM crack would cut across the center of a row of elements in the middle of the specimen, Figure 2. The entire model was enriched, enabling the propagation of the pre-defined XFEM crack. The crack propagation direction was set parallel to the global direction 1.

In the XFEM-CS approach, as mentioned in Section 2, the quadratic stress interaction criterion (Equation 1) was chosen as the damage initiation criterion. The maximum tractions, $t_n^0 = 60$ MPa, and $t_s^0 = t_t^0 = 90$ MPa, were obtained from (Hallet, 2009), however no accepted standard is available for determining these values. Further, a bi-linear traction-separation law was chosen and the mixed mode response was given by the BK criterion with $G_n^c = G_{Ic} = 0.17$ kJ/m^2, and $G_s^c = G_{IIc} = G_{IIIc} = 0.5$ kJ/m^2 and $\eta = 1.47$ taken from the original benchmark paper (Krueger, 2008). Note that in the DCB case, the crack is loaded in Mode I, and therefore the choice of mixed-mode criterion should not have any bearing on the solution. Damage stabilization was used for all analyses with a viscosity coefficient equal to $1\text{E}-5$ unless otherwise stated.

For the XFEM-VCCT approach, since an initial XFEM crack is present in the model, only the definition of the fracture criterion is needed. The latter was also chosen to be the BK criterion and was defined as described above. To aid convergence, a viscosity coefficient equal to $1\text{E}-5$ was used for all analyses. The remaining options were kept to their default values.

All the analyses performed were linear, with maximum and minimum time steps defined as, $t_{max} = 0.05$ and $t_{min} = 1\text{E}-15$, respectively. The solution controls were not changed from their default values, except for the maximum number of cut-backs allowed in an increment, which was increased to 50. Finally, the displacement prescribed was set to $V = 2$ mm.

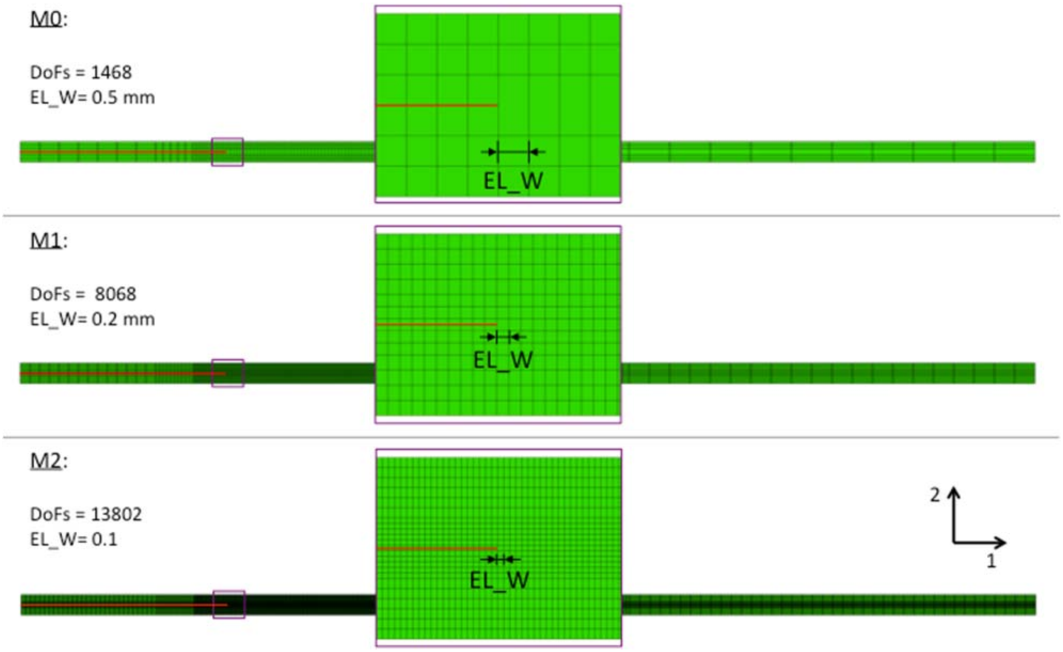

Figure 2. XFEM initial crack definition and mesh refinements used to model the DCB specimen.

3.3 Results

3.3.1 XFEM-VCCT

Figure 3a) compares the results obtained using the XFEM-VCCT approach with increasing mesh refinement to the benchmark results. Results show that XFEM-VCCT does not converge to the benchmark, with very little difference between mesh refinements M1 and M2. The effect of the type of element was also assessed, Figure 3b). Models created with element types CPE4I (Incompatible Modes), and CPE4R (Reduced Integration) seem to provide better results than models created with the standard CPE4 (Full integration, 4 integration points) element.

3.3.2 XFEM-CS

Figure 4a) compares the results obtained using XFEM-CS with increasing mesh refinement to the benchmark results. In contrast to the XFEM-VCCT approach, XFEM-CS shows a convergent behavior, Figure 4a). Regarding the element type, models created with CPE4I and CPE4R type elements give the best results, Figure 4b). In Figure 5a), the option '**`position = cracktip`**', see Section 2, is evaluated for element types CPE4I and CPE4. Results show that this option provides an improvement in accuracy for both element types. The effect of different stabilization values was also assessed and is illustrated in Figure 5b), showing that a viscosity coefficient greater than $1E-4$ leads to a significant compromise in accuracy.

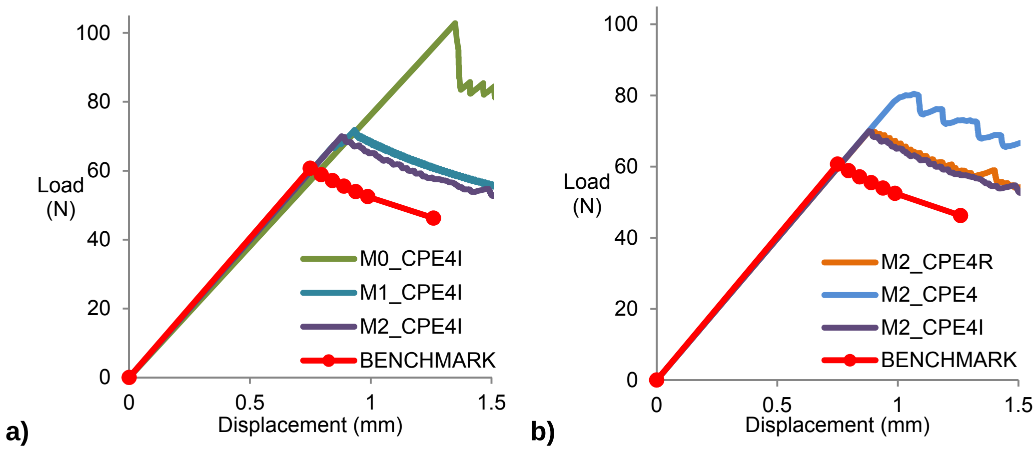

Figure 3. Effect of mesh refinement (a), and element type (b) in the modeling of a DCB specimen using the XFEM-VCCT approach.

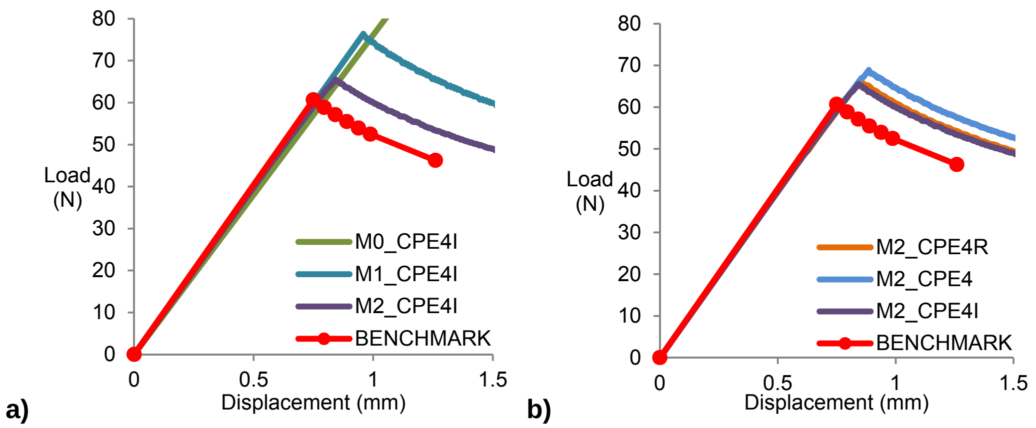

Figure 4. Effect of mesh refinement (a), and of element type (b) in the modeling of the DCB specimen using the XFEM-CS approach.

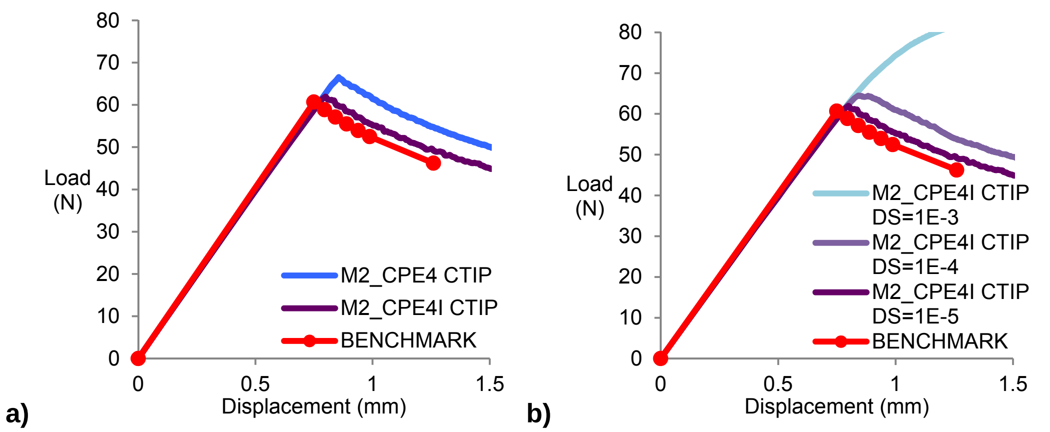

Figure 5. Effect of the option 'position = cracktip', labeled 'CTIP' (a), and of the damage stabilization (b) on the modeling of the DCB specimen using the XFEM-CS approach.

4. XFEM assessment: MMB Benchmark

Figure 6 illustrates the numerical model, dimensions, boundary conditions and material properties used to obtain the mixed-mode MMB benchmark (Krueger, 2012). In the present work, a single mixed mode ratio was used, $G_{II}/G_T = 0.5$.

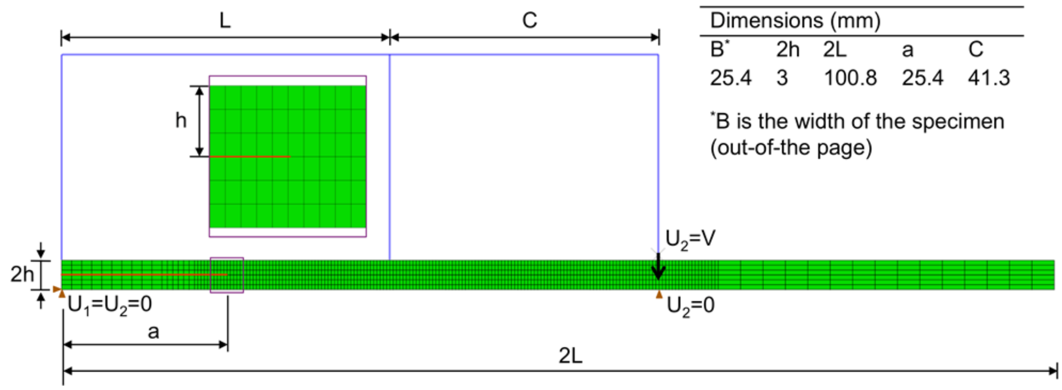

Dimensions (mm)				
B*	2h	2L	a	C
25.4	3	100.8	25.4	41.3

*B is the width of the specimen (out-of-the page)

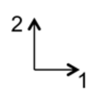

Material Properties, IM7/8552:

E_{11} (MPa)	$E_{22} = E_{33}$ (MPa)	$G_{12} = G_{13}$ (MPa)	G_{23} (MPa)	$\nu_{12} = \nu_{13}$	ν_{23}	G_{Ic} (kJ/m²)	G_{IIc} (kJ/m²)	η**
161	11.38	5.2	3.9	0.32	0.45	0.212	0.774	2.1

**Exponent used in the BK mixed-mode fracture criterion

Figure 6. Numerical model, dimensions and material properties used to obtain the MMB benchmark curve for G_{II}/G_T = 0.5, (Krueger, 2012).

The MMB benchmark was created in a similar way to the DCB benchmark. Several two-dimensional finite element models were used to simulate specimens with different delamination lengths. For each delamination length, load and the displacement were recorded. The total strain energy release rate, G_T, is calculated for a fixed applied displacement. In the mixed mode case, delamination is assumed to propagate when the computed energy release rate, G_T, equals G_c, given by the BK criterion, Equation 2, with $G_n^c = G_{Ic}$ and $G_s^c = G_{IIc}$. Similar to the DCB benchmark, the critical loads and displacements for each delamination length are calculated from Equation 3. As before, the path connecting the critical values in a load/displacement plot is defined as the benchmark. It is assumed that during the automated propagation, the analysis has to follow the critical path. More details of the MMB benchmark development and the assessment of the mixed-mode propagation capabilities using the VCCT implementation in Abaqus are presented in (Krueger, 2012).

4.1 XFEM MMB

Figure 7 shows three models with increasing mesh refinement, M0 to M2, used to assess the performance of XFEM as implemented in Abaqus/Standard 6.13. Their dimensions, boundary conditions and material properties are identical to those used in the benchmark, Figure 6. As in the DCB case, the initial XFEM crack and mesh were defined such that the XFEM crack would cut across the center of a row of elements in the middle of the specimen, Figure 7.

In the XFEM-CS approach, as in the DCB case, the quadratic stress interaction criterion was chosen as the damage initiation criterion, Equation 1, with $t_n^0 = 60$ MPa, and $t_s^0 = t_t^0 = 90$ MPa, (Hallet, 2009). Further, a standard bi-linear traction-separation law was chosen and the mixed mode response was given by the BK criterion defined with $G_n^c = G_{Ic} = 0.212\ \mathrm{kJ/m^2}$, and $G_s^c = G_{IIc} = G_{IIIc} = 0.774\ \mathrm{kJ/m^2}$ and $\eta = 2.1$, the same criterion used to obtain the benchmark (Krueger 2012). Damage stabilization with a viscosity coefficient equal to $1\mathrm{E}-5$ was used in all analyses, unless otherwise stated.

For the XFEM-VCCT approach, the fracture criterion was also chosen to be the BK criterion and was defined as described above. To aid convergence, a viscosity coefficient of $1\mathrm{E}-5$ was used in all analyses.

All the analyses performed were linear, with maximum and minimum time steps defined as, $t_{max} = 0.05$ and $t_{min} = 1\mathrm{E}-15$, respectively. The solution controls were not changed from their default values, except for the maximum number of cut-backs allowed in an increment, which was increased to 50. Finally, the displacement prescribed to the load fixture, modeled with rigid links, was $V = -5$ mm.

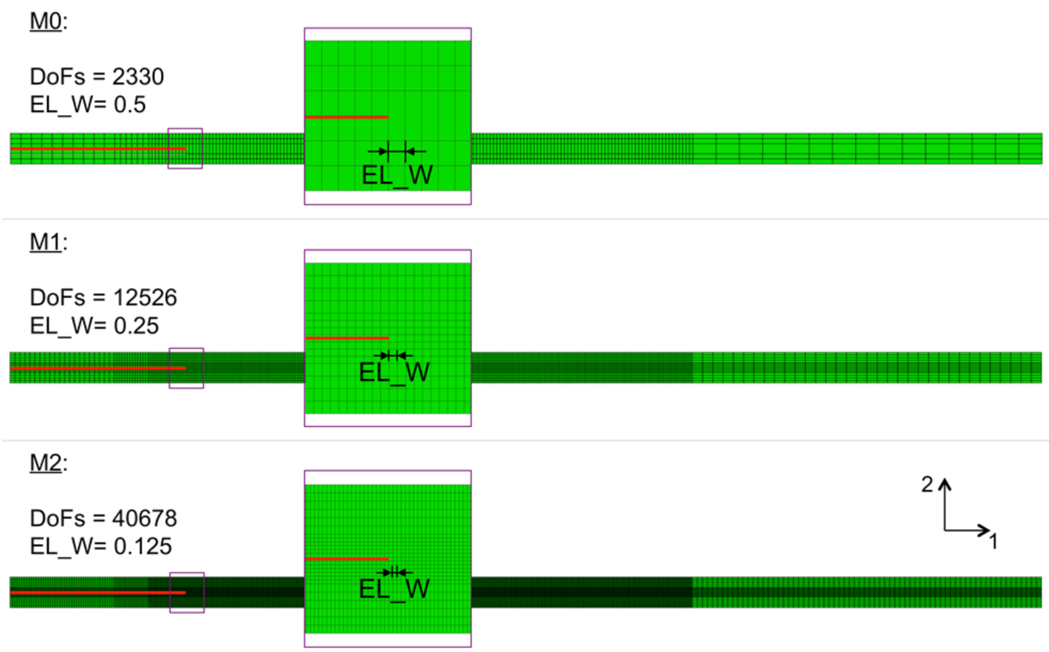

Figure 7. XFEM initial crack definition and mesh refinements used to model the MMB specimen.

4.2 Results

4.2.1 XFEM-VCCT

Figure 8a) compares the results obtained using the XFEM-VCCT approach with increasing mesh refinement to the benchmark results. As in the DCB case, the results obtained do not converge with mesh refinement. Indeed, the most refined mesh has the worse performance. Regarding the type of element, models created with CPE4I and CPE4R type elements provide the best results.

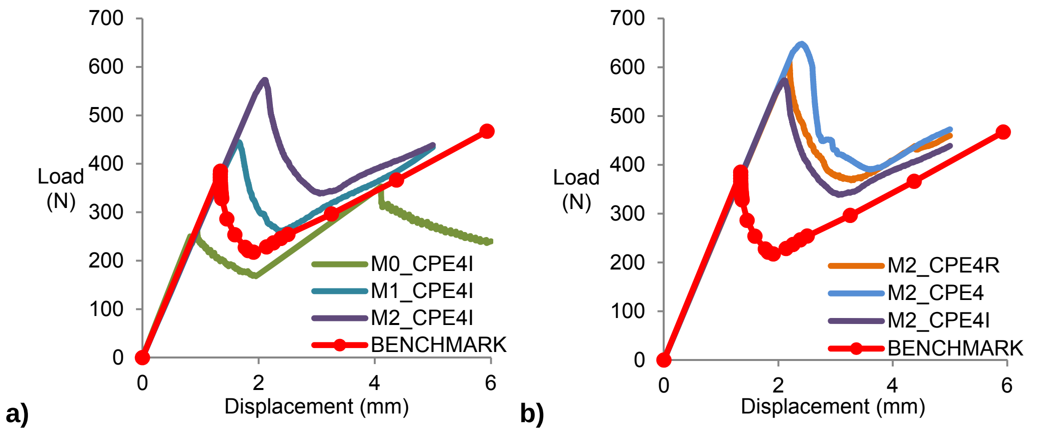

Figure 8. Effect of mesh refinement, and (b) element type on modeling of an MMB specimen using the XFEM-VCCT approach.

4.2.2 XFEM-CS

Figure 9a) compares the results obtained using XFEM-CS with increasing mesh refinement to the benchmark results. The XFEM-CS approach shows a convergent behavior, Figure 9a). Regarding the element type, models created with CPE4I type elements yield more accurate results, followed by results obtained from models created with CPE4R type elements, Figure 9b). When using the option ‘position = cracktip’, the benchmark can be closely followed when using the model with the finest mesh, ‘M2’, created either with CPE4I or CPE4 type elements, Figure 10a). Finally, Figure 10b) shows that stabilization values greater than $1\mathrm{E}-4$ lead to a significant compromise in accuracy.

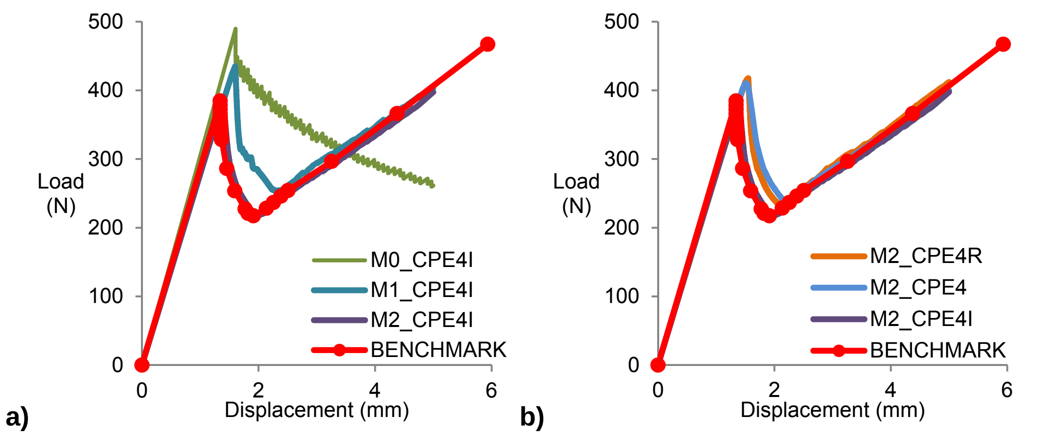

Figure 9. Effect of mesh refinement (a), and element type (b) in the modeling of the MMB specimen using the XFEM-CS approach.

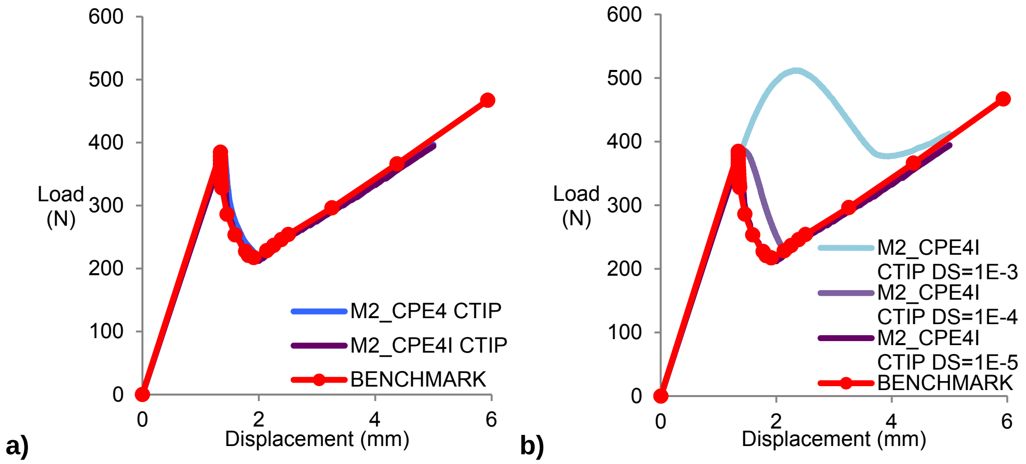

Figure 10 Effect of the option 'position = cracktip' labeled 'CTIP' (a), and damage stabilization (b) on the modeling of the MMB specimen using the XFEM-CZ approach.

5. Modeling Delamination Migration (DM) test

The DM test was proposed in (Ratcliffe, 2012), and consists of a cross-ply specimen beam clamped at both ends. A Teflon insert acts as an artificial delamination at an interface between a 0° ply (specimen span direction, Figure 11) and a stack of four 90° plies. The specimen can be loaded in a manner that leads to delamination growth from the Teflon insert which eventually migrates through the stack of 90° plies to another ply interface. This test has been successfully modeled using the Floating Node Method (FNM) combined with VCCT and a physics-based migration criterion as discussed in detail in (De Carvalho, 2013).

The dimensions and boundary conditions of the numerical model used in the present work are given in Figure 11. The material used was IM7/8552, whose properties are given in Figure 6. Two types of damage mechanisms interact in this specimen: i) delamination, and ii) matrix cracking. In the strategy proposed, delamination is modeled using a Cohesive Surface (CS), while the matrix cracking is captured using XFEM.

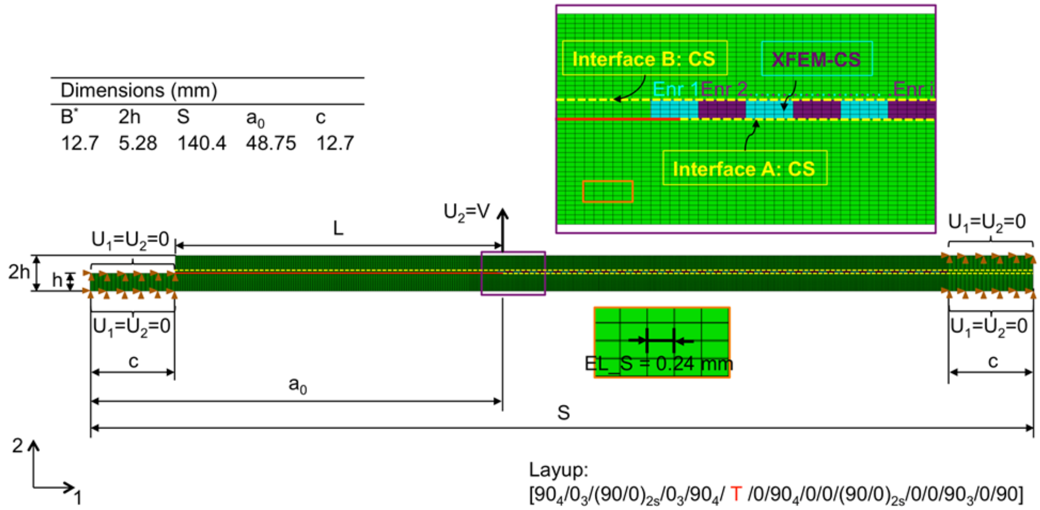

Figure 11. Delamination migration numerical model.

5.1 Preliminary runs and model definition

A number of preliminary analyses were performed, to help define an overall strategy that could predict delamination migration. For brevity, the results from these attempts and their implications to the final strategy used are summarized in this section.

5.1.1 Mesh refinement

The initial mesh refinement was chosen based on the findings from Section 2. The refinement through-the-thickness was set to one element per ply. This choice would allow a square element to have a length along the span of the specimen of EL_S = 0.12 mm, approximately the same size used in the most refined meshes in Sections 3 and 4. However, despite various attempts, migration could not be obtained with this mesh. Depending on the options and elements used, the analyses would either: (i) not converge, or (ii) not predict migration. Convergence issues were often caused by the interaction between matrix cracks and the delamination propagating from the initial crack. In cases where analyses completed but migration was not predicted, the matrix cracks often arrested at a corner of an element, suggesting their position relative to the mesh could affect the solution. Indeed this proved to be the case, as doubling the elements width gave significantly different (better) results. Therefore, in the remainder of this work, the elements located ahead of the crack tip have a length EL_S = 0.24 mm, Figure 11. However, this observation indicates that the method is dependent on the mesh and the results do not necessarily converge to the physical solution with mesh refinement. Additionally, clear guidelines for the optimal refinement level/element size cannot be defined, as it is unlikely that the solution adopted in the present study also holds in a general case.

5.1.2 Cohesive surface (CS) and VCCT

To model the initial delamination from the Teflon insert two techniques were used: cohesive surface, here named CS, and VCCT. When comparing to experimental observations, the results computed when using VCCT were, in general, inferior to those obtained using CS in the simulations. This poor agreement was caused by the interaction between matrix cracks and the delamination as it grew from the insert, prior to migration. This interaction led to a strong stick-slip response as the delamination grew. When using CS in the simulation, this interaction was in general less pronounced and did not significantly affect the solution. Therefore, in the present work, only results obtained with CS are shown. For CS, damage initiation was defined through a quadratic stress criterion, Equation 1, with $t_n^0 = 60$ MPa, and $t_s^0 = t_t^0 = 90$ MPa, (Hallet, 2009). The traction-separation response was modeled using a standard bi-linear law with mixed mode response defined by the BK criterion, Equation 2, with required material properties given in Figure 6.

5.1.3 Enrichment areas

As it will be shown next, in the approach proposed, matrix cracks are triggered from the onset of the delamination. These initial matrix cracks, however, do not propagate, and do not lead to migration, as shown in detail A of Figure 12. Therefore, if only one enriched area is used, the onset of a single matrix crack inhibits the onset of further cracks as the delamination grows since Abaqus/Standard allows only one crack per enrichment area. This limitation can prevent migration from being captured. To circumvent this issue, multiple enrichment areas with 5 elements each are defined along the element span ahead of the pre-crack, Figure 11, enabling multiple cracks to initiate as the delamination grows. This need for prescribing multiple enrichment areas, and their location, shares similarities with other more conventional strategies such as the one proposed in (Hallet, 2009), where the location of matrix cracks is decided prior to the simulation. This can be seen as a limitation of the method, since the user needs to know beforehand, how and where to enrich the numerical model, to capture the correct damage morphology.

5.1.4 XFEM approach and element type

The XFEM-CS approach was chosen to capture the matrix cracks, since it is significantly more accurate than XFEM-VCCT, as demonstrated in Sections 3 and 4. Damage initiation is captured using a maximum principal stress criterion, with $\sigma_{max} = Y_T = 73$ MPa (Kadour, 2007), which also provides matrix crack orientation. The propagation was modeled using a standard bi-linear law with a mixed mode response defined using the BK criterion, Equation 3. The intralaminar fracture toughness values for matrix cracking were assumed to be the same as the interlaminar fracture toughness values for the material given in Figure 6, (Czabaj, 2012).

Results from Sections 3 and 4 also suggest that element CPE4I combined with the option '**`position = cracktip`**' provide the most accurate results. However, preliminary analysis showed that this combination led to convergence issues. Alternatively, the second best option was used, full integration elements CPE4, combined with the option '**`position = cracktip`**'.

5.2 Results

Four models with different load offsets L (Figure 11) were analyzed. Large displacement formulation (`*Step,…, nlgeom=YES`) was used for all analyses, with maximum and minimum time steps of $t_{max} = 0.05$, and $t_{min} = 1\text{E} - 15$, respectively. Stabilization with a viscosity coefficient of $1\text{E} - 5$ was used both in the XFEM-CS and in the Cohesive Surfaces (CS) defined along interfaces A and B, see Figure 11.

In general the computed results show a good qualitative agreement with experimental observations as shown in Fig. 12. Qualitatively, the main difference is the presence of matrix cracks in the simulations. These matrix cracks, with negative slope in the 1-2 plane, form prior to migration however are not present in the experiments, see Figure 12, detail A. Additionally, the smooth transition from the delamination to the matrix crack is not captured correctly, Figure 12 detail B. Quantitatively, the load-displacement plots show good agreement, Figure 13. The mismatch in the initial stiffness is likely due to boundary conditions and/or material properties and is currently under investigation. Overall, the maximum load is well predicted. For cases (a) and (b), the simulations predicted arrest after migration. This was not observed in the experiments. For case (a), delamination arrest was observed to occur before the migration event, while in case (b) both delamination and migration occurred during the same unstable event. For cases (c) and (d), simulations predict a region of stable delamination growth, which can be correlated to a series of small unstable events, prior to the main load drop, observed in the experiments. Also, the migration location, Δ_{K}, is in general well predicted as shown in Figure 14, where the distance from the load application point to the migration location, Δ_{K}, is plotted versus the normalized load offset L/a_0.

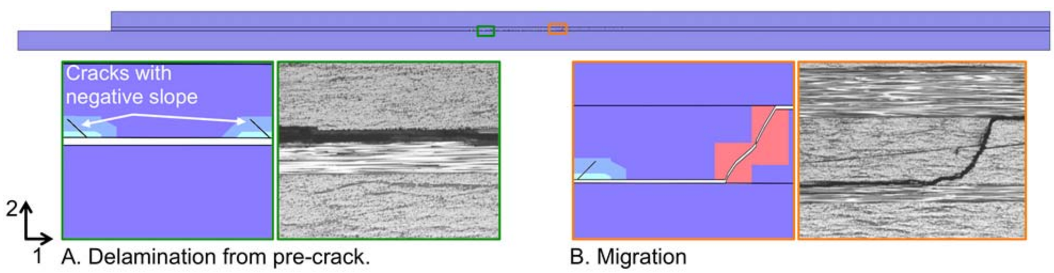

Figure 12 Qualitative comparison between simulation and experiments.

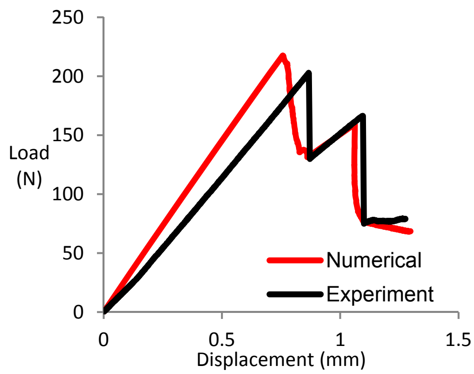

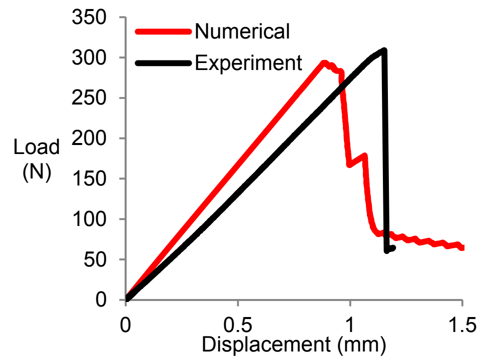

a) $L = a_0$ **b)** $L = 1.1a_0$

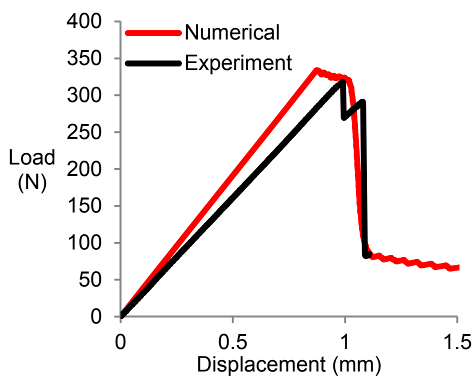

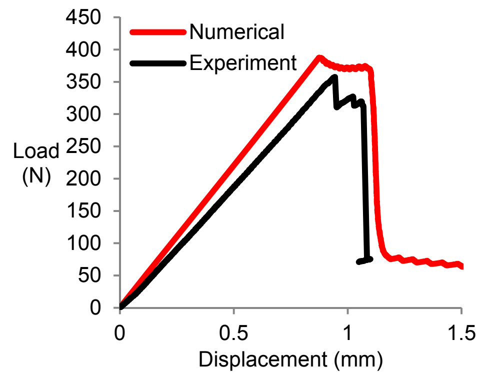

c) $L = 1.2a_0$ **d)** $L = 1.3a_0$

Figure 13 Experimental and predicted load-displacement plots.

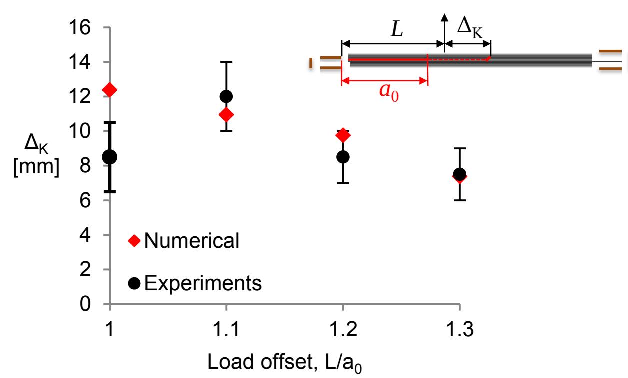

Figure 14 Migration location.

6. Discussion

The present study shows that the current implementation of XFEM-VCCT in Abaqus/Standard 6.13 is not yet capable of following the DCB and MMB benchmarks with a good level of accuracy. Regarding XFEM-CS, results show that a good level of accuracy can be obtained, provided the mesh is sufficiently refined. The most accurate results are obtained using the option '`position = cracktip`', where models created with CPE4I elements yielded the best results, followed by models created with CPE4 elements. As expected, stabilization affects the solution, and should be used with care, with viscosity coefficients greater than $1\mathrm{E}-4$ significantly affecting the solution.

It can be argued that there is a range of problems where both XFEM-CS and XFEM-VCCT can be used. In these problems, XFEM-CS provides an obvious alternative to the less accurate XFEM-VCCT implementation. However, there are problems where XFEM-CS cannot yet be applied. One such class of problems is the simulation of crack growth under fatigue loading, where XFEM-VCCT could provide an invaluable tool. Therefore, further improvement of the XFEM-VCCT implementation is highly desirable.

The strategy proposed for the interaction of delamination propagation and matrix cracks is capable of simulating the delamination migration test. Qualitatively, the main difference is the presence of matrix cracks, with negative slope in the 1-2 plane, which are not seen in the experiments. Nevertheless, the presence of these cracks does not seem to significantly affect the solution, if CS is used to model delamination. Additionally, also the shape of the crack as it migrates is not completely captured. Quantitatively, both load-displacement plots and migration location show good agreement with experiments. Nevertheless, one of the major limitations is the strong dependency of the solution on small variations of the mesh, as mentioned in Section 5.1. Furthermore, results do not converge with refinement, as migration could not be predicted with a more refined (structured) mesh. Additionally, the requirement of pre-defining the number and position of the enrichment zones is considered a limitation, as the user might not always know beforehand what damage morphology to expect.

7. Conclusions

Comparison with previously published benchmark solutions has shown that the XFEM-CS approach is significantly more accurate than the XFEM-VCCT. Using XFEM-CS with '`position = cracktip`' and element type CPE4I provided the most accurate results.

A strategy is proposed that is capable of simulating the delamination migration test. Good qualitative and quantitative agreement is achieved. The approach has three main limitations: i) very sensitive to small variations in mesh, ii) not convergent with refinement, iii) definition of enrichment zones requires 'a priori' knowledge of the solution. Nevertheless, the results obtained are encouraging, suggesting XFEM combined with existing approaches can become a key technology for the high-fidelity simulation of damage initiation and propagation in composite materials.

8. References

1. Belytschko, T. and T. Black, "Elastic Crack Growth in Finite Elements with Minimal Remeshing," International Journal for Numerical Methods in Engineering, Vol. 45, pp. 601-620, 1999.
2. Benzeggagh, M. L. and Kenane, M., "Measurement of Mixed-Mode Delamination Fracture Toughness of Unidirectional Glass/Epoxy Composites with Mixed-Mode Bending Apparatus," Composites Science and Technology, vol. 56, pp. 439-449, 1996.
3. Czabaj, M. W. and Ratcliffe, J. G., "Comparison of Intralaminar and Interlaminar Mode-I Fracture Thoughness of Unidirectional IM7/8552 Graphite/Epoxy Composite," Proceedings of the American Society for Composites – Twenty-Seventh Technical Conference, Arlington, TX, USA, paper 114, 2012.
4. De Carvalho, N. V., Chen, B. Y., Pinho, S. T., Baiz, P. M., Ratcliffe, J. G., Tay, T. E., "Floating Node Method and Virtual Crack Closure Technique for Modeling Matrix Cracking Delamination Migration," 19th International Conference on Composite Materials, Montreal, 2013.
5. Hallet, S. R., Green, B. G., Jiang, W. G., Cheung, K. H., Wisnom, M. R. "The Open Hole Tensile Test: a Challenge for Virtual Testing of Composites," International Journal of Fracture, Vol. 158, No. 2, pp. 169-181, 2009.
6. Kaddour, A. S. and Hinton, M. J., "Instructions to Contributors of the Second World-Wide Failure Exercise (WWFE-II): Part (A)," 2007.
7. Krueger, R., "An Approach to Assess Delamination Propagation Simulation Capabilities in Commercial Finite Element Codes," NASA/TM-2008-215123, 2008.
8. Krueger, R., "Development and Application of Benchmark Examples for Mixed-Mode I/II Quasi-Static Delamination Propagation Predictions," NASA/CR-2012-217562, 2012.
9. Ratcliffe, J., Czabaj, M. W. and O'Brien, T. K., "Characterizing Delamination Migration in Carbon/Epoxy Tape Laminates," Proceedings of the American Society for Composites Twenty-Seventh Technical Conference, Arlington, TX, USA, paper 313, 2012.
10. Song, J. H., Areias, P. M. A. and Belytschko, T., "A Method for Dynamic Crack and Shear Band Propagation with Phantom Nodes," International Journal for Numerical Methods in Engineering, vol. 67, pp 868–893, 2006.

9. Acknowledgements

The authors would like to thank James Ratcliffe (National Institute of Aerospace), Mike Sasdelli (Dassault Systèmes) and Rassin Grantab (Dassault Systèmes) for the helpful discussions.